

Manuscript Number:

Title: Dynamic modeling of a PV pumping system with special consideration on water demand

Article Type: Special Issue: ICAE2012

Keywords: renewable energy resources, solar energy, photovoltaic system, pumping system, water demand

Corresponding Author: Mr. Pietro Elia Campana,

Corresponding Author's Institution:

First Author: Pietro Elia Campana

Order of Authors: Pietro Elia Campana; Hailong Li; Jinyue Yan

Abstract: The exploitation of solar energy in remote areas through photovoltaic (PV) systems is an attractive solution for water pumping for irrigation systems. The design of a photovoltaic water pumping system (PVWPS) strictly depends on the estimation of the crop water requirements and land use since the water demand varies during the watering season and the solar irradiation changes time by time. It is of significance to conduct dynamic simulations in order to achieve the successful and optimal design. The aim of this paper is to develop a dynamic modeling tool for the design of a of photovoltaic water pumping system by combining the models of the water demand, the solar PV power and the pumping system, which can be used to validate the design procedure in terms of matching between water demand and water supply. Both alternate current (AC) and direct current (DC) pumps and both fixed and two-axis tracking PV array were analyzed. The tool has been applied in a case study. Results show that it has the ability to do rapid design and optimization of PV water pumping system by reducing the power peak and selecting the proper devices from both technical and economic viewpoints. Among the different alternatives considered in this study, the AC fixed system represented the best cost effective solution.

Referees

1. Han Song

PhD student

School of Sustainable Development of Society and Technology, Mälardalen University,
SE-72123 Västerås, Sweden

song.han@mdh.se

2. Umberto Desideri

Professor

Department of Industrial Engineering, University of Perugia, Via G. Duranti 93 -
06125 Perugia, Italy

umberto.desideri@unipg.it

3. Takeshita Takayuki

Project Lecturer

The University of Tokyo

takeshita@ir3s.u-tokyo.ac.jp

umberto.desideri@unipg.it

Highlights

1. Evaluation of water demand and solar energy is essential for PV pumping system.
2. The design for a PV water pumping system has been optimized based on dynamic simulations
3. It is important to conduct dynamic simulations to check the matching between water demand and water supply.
4. AC pump driven by the fixed PV array is the most cost-effective solution.

1 DYNAMIC MODELING OF A PV PUMPING SYSTEM WITH SPECIAL CONSIDERATION ON WATER DEMAND

2 Pietro Elia Campana^{1*}, Hailong Li¹, Jinyue Yan^{1,2*}

3 ¹School of Sustainable Development of Society and Technology, Mälardalen University, SE-72123 Västerås,
4 Sweden

5 ²School of Chemical Science, Royal Institute of Technology, SE-144 Stockholm, Sweden

6

7 **ABSTRACT**

8 The exploitation of solar energy in remote areas through photovoltaic (PV) systems is an attractive solution for
9 water pumping for irrigation systems. The design of a photovoltaic water pumping system (PVWPS) strictly
10 depends on the estimation of the crop water requirements and land use since the water demand varies during
11 the watering season and the solar irradiation changes time by time. It is of significance to conduct dynamic
12 simulations in order to achieve the successful and optimal design. The aim of this paper is to develop a dynamic
13 modeling tool for the design of a of photovoltaic water pumping system by combining the models of the water
14 demand, the solar PV power and the pumping system, which can be used to validate the design procedure in
15 terms of matching between water demand and water supply. Both alternate current (AC) and direct current (DC)
16 pumps and both fixed and two-axis tracking PV array were analyzed. The tool has been applied in a case study.
17 Results show that it has the ability to do rapid design and optimization of PV water pumping system by reducing
18 the power peak and selecting the proper devices from both technical and economic viewpoints. Among the
19 different alternatives considered in this study, the AC fixed system represented the best cost effective solution.

20

21 **Keywords:** renewable energy resources, solar energy, photovoltaic system, pumping system, water demand.

22

23

24

25

26

27

28

29

30

31

32

33 **NOMENCLATURE**

34 *Abbreviation*

35	AC	Alternate current
36	DC	Direct current
37	ICC	Initial investment cost
38	MPPT	Maximum power point tracker
39	PV	Photovoltaic
40	PVWPS	Photovoltaic water pumping system
41	SCS	Soil conservation service

42

43 *Symbols*

44	e_a	Actual vapour pressure [kPa]
45	E_h	Hydraulic energy [kWh/day]
46	e_s	Saturation vapour pressure [kPa]
47	ET_0	Reference evapotranspiration [mm/day]
48	ET_c	Evapotranspiration in cultural conditions [mm/day]
49	EX	Extraterrestrial radiation (kWh/m ²)
50	g	Gravity acceleration [m/s ²]
51	G	Soil heat flux density [MJ/m ² day]
52	GH	Global horizontal radiation (kWh/m ²)
53	H	Total dynamic head [m]
54	I_b	Beam radiation [Wh/m ²]
55	I_d	Diffuse radiation [Wh/m ²]
56	I_{tot}	Global radiation on the array [Wh/m ²]
57	$I_{tot,d}$	Daily total radiation [kWh/m ² /day]
58	$K_b(\theta)$	Incidence angle modifier
59	K_c	Cultural coefficient
60	K_d	Incidence modifier for diffuse radiation
61	LI	Longwave incoming radiation (kWh/m ²)
62	LO	Longwave outgoing radiation (kWh/m ²)
63	NOCT	Nominal operating cell temperature [°C]
64	P	Precipitation (mm)
65	$P(T,\theta)$	Power output [W]
66	Q	Water flow [l/s]
67	RH	Relative humidity (%)

68	R_n	Net radiation at crop surface [MJ/m ² day]
69	T	Temperature [°C]
70	T_a	Ambient temperature [°C]
71	T_c	Cell temperature [°C]
72	T_r	Reference temperature [°C]
73	u_2	Wind speed at 2 m height [m/s]
74	W_g	Water gross volume [mm/day]
75	WS	Wind speed (m/s)
76	W_t	Watered height [mm]
77	α	Power temperature coefficient [%/°C]
78	γ	Psychrometric constant [kPa/°C]
79	Δ	Slope vapour pressure curve [kPa/°C]
80	η_{ob}	Optical efficiency for beam radiation [%]
81	η_s	System efficiency [%]
82	η_p	Pump efficiency [%]
83	$\eta_{PV,T}$	PV module thermal efficiency [%]
84	η_w	Electric wires efficiency [%]
85	Θ	Angle of incidence [°]
86	ρ	Water density [kg/m ³]

87 **1. INTRODUCTION**

88 The availability of electricity in remote areas is one of the main issues regarding the design and operation of
89 irrigation systems. Nevertheless, it is quite common in the developing countries that the access to the electric grid
90 is unavailable. With the development of photovoltaic (PV) technology that can convert the solar energy to
91 electricity, using PV cells has become a more attractive solution to provide the required power for the water
92 pumping system, especially in the areas that have abundant solar energy resources [1]. The high technical
93 reliability of PVWPSs for irrigation purposes, their long term economic viability and recent developments as well
94 as the weaknesses have been shown by several studies and field experiences. The knowledge and the
95 competencies achieved in this field resulted as starting point and recommendations for further and future
96 programmes worldwide [2, 3]. For example, in 2009 the Government of Bangladesh has set as target for 2014 to
97 install more than 10000 PVWPS for irrigation with a total installed capacity of 10 MW_p. Only in 2010 India has
98 installed more than 50 MW_p PV off-grid systems of which pumping system represent a large part [4].

99 Many studies have been carried out in the development of the PVWPS focusing on the system sizing, system
100 modeling, economic performance and environmental feasibility. Models have been presented for the estimation
101 of water demand [5, 6], assessment of the solar energy [7, 8], PV generator and controller [8, 9] and for the
102 motor-pump system [10]. Some demonstration projects that link the power output from the photovoltaic

103 generator, pumping system power consumption and instantaneous water flow output have been conducted [11].
104 Based on the available models, the approaches regarding the system optimization have been developed [12]. In
105 addition, economic and environmental evaluations showed the feasibility of photovoltaic pumping system
106 compared to traditional systems driven by diesel engines [13].

107 The main R&D gaps for the implementation of the PVWPSs exist not only in the technologies of PV and pump.
108 Problems related to the local peculiarity need to be considered [14]. The local peculiarity includes water
109 resources availability, water demand, different pumping system configurations, acceptance and management of
110 the system. These issues need to be investigated in order to achieve the success of a photovoltaic pumping
111 project. In addition, in the current state of the art the capital cost of a PVWPS is still higher than the traditional
112 system driven by diesel engine, which is considered as the major barrier for the large scale commercialization,
113 although the operation costs are much lower. Therefore, as regards the optimization, efforts are mainly focused
114 on minimizing the cost.

115 Dynamic operation is one of the most important characteristics of the PVWP systems. Due to the dynamic
116 variation of solar irradiation and the precipitation, the PV power output and the water demand of irrigation vary
117 time by time. Meanwhile, as the solar irradiation varies, the dynamic PV power output would affect the
118 performance of pump, resulting in a dynamic variation of pump efficiency and power consumption. In order to
119 achieve the successful and optimal design and minimize the costs, the system dynamic characteristic has to be
120 considered. The impacts of the dynamic variation of solar irradiation on the dynamic variation of water demand
121 and pump performance have been investigated thoroughly. The objective of this paper is to develop a dynamic
122 simulation tool and conduct dynamic simulations for a PVWP system, by integrating all of the dynamic variations
123 of water demand, solar irradiation, PV power output and pump performances. Both AC and DC pump and both
124 fixed and two-axis sun tracking systems were investigated from a technical and economic viewpoint. A dynamic
125 water demand model was developed based on the local climatic conditions, soil characteristics and type of crops.
126 With the predicted dynamic water demand the instant performances of PVWP system were studied. Such a
127 dynamic simulation can be used to evaluate the existing design, checking if there is mismatch between the
128 pumped water and the demanded water. The results would also give some guidelines or suggestion concerning
129 system optimization from the perspective of dynamic water demand.

130 **2. DESCRIPTION OF THE SYSTEM**

131 A PVWPS is basically composed of a PV array, a power controlling system and a pumping system connected to
132 the distribution system that can be a water tank or directly an irrigation system. A schematic diagram of the
133 photovoltaic water pumping system studied in this work and the related models adopted is presented in Figure 1.
134 The photovoltaic array consists of photovoltaic modules that are connected in series or in parallel depending on
135 the voltage and current output requirements. In this work both fixed and two-axis sun tracking systems were
136 investigated and compared technically and economically. The power controlling system is an interface between
137 the PV modules and the motor-pump system with the function to improve the coupling performances. The power

138 conditioning system can be a DC/DC converter or a DC/AC inverter depending on the motor-pump technology.
139 Both converter and inverter are usually equipped with a maximum power point tracker (MPPT) device in order to
140 maximize the power extraction from the solar array. In this study, both multistage centrifugal DC and AC pump
141 and the related power controllers were adopted in order to investigate and compare the performances, especially
142 in terms of power consumption, water pumped and costs.

143
144 **Figure 1: Schematic diagram of a photovoltaic water pumping system.**

145 **3. METHODOLOGY**

146 This study is divided into three parts: the estimation of the water demand for irrigation, the assessment of the
147 exploitable solar energy and related power output from the PV array, and sizing and dynamic modeling of the
148 system. The assessment of water demand depends on a lot of factors such as the type of crop, type of soil,
149 irrigated area, rainfall regime, average temperatures, wind speed and solar radiation. Here the FAO Penman-
150 Monteith method was used to estimate the water demand for growing Alfalfa (*Medicago Sativa*) in a sandy soil
151 with some assumptions regarding the soil characteristics [5]. Based on this model both the assessment of the
152 monthly water demand that is the input data for the design procedure, and the hourly water demand used in the
153 dynamic modeling can be obtained. The assessment of the solar energy available and power output from the
154 solar array was made on the basis of data provided by a global climatic database and processed by the program
155 WINSUN considering different tilt angles and system configurations [7, 8]. The design process was carried out
156 through the estimation of the water demand and hydraulic head for growing Alfalfa in order to estimate the
157 power of the pumping system. The PV array power peak was then calculated on the basis of the daily required
158 hydraulic energy, daily collectable solar energy and system efficiency. The worst conditions in terms of available
159 solar energy and required water demand were chosen for the design procedure. The dynamic modeling of the
160 photovoltaic water pumping system was used to prove and optimize the sizing process, underlining the match
161 between water demand and water supply. A describing flow chart of the designing process and dynamic
162 simulations carried out in this paper and the related parameters affecting both processes are presented in Figure
163 2.

164
165 **Figure 2: Designing and dynamic modeling procedure.**

166
167
168 The dynamic simulations were done based on the hourly data of solar radiation, angle of incidence and
169 temperature in order to estimate the hourly power output from the PV array. The PV power output was then
170 used to estimate the hourly water output of the pumping system according to the power input-instantaneous
171 flow characteristic curve of the chosen pumps and power controller efficiency. The match between water supply
172 and water demand was analyzed using the results achieved by the hourly dynamic modeling of water pumped
173 and estimated water requirements on monthly basis. The economic analysis carried out in this work was mainly

174 focused on the differences in initial capital costs between system equipped with AC and DC pump, fixed PV array
 175 and sun tracking array. The economic investigation was based on the prices referring to the Chinese market and
 176 taken from an on-line business-to-business trading platform [15].

177 **3.1 Climatic data**

178 The site chosen for this study was in Xining, the capital city of Qinghai Province, China, located on the eastern
 179 edge of the Qinghai-Tibet Plateau (Latitude: 36°37' N; Longitude: 101°46' E; Altitude: 2275 m a.s.l.). This location
 180 is featured by a continental cold semi-arid climate with high potential in solar energy. The monthly daily average
 181 temperatures range from -6.0°C in January up to 22.2°C in July. The annual precipitation is 269 mm and is mainly
 182 distributed between May and September. The annual global radiation on horizontal plane is 1542 kWh/m² with
 183 2701 sunshine hours. The climatic data referring to Xining were taken from the global database provided by
 184 Meteonorm including temperature, relative humidity, precipitation, wind speed, global radiation on a horizontal
 185 plane, extraterrestrial radiation, incoming and outgoing longwave radiation as given in Table 1 [7]. The monthly
 186 statistical data were used for the estimation of the monthly average daily water demand and the sizing of the
 187 PVWPS. Whereas the hourly data elaborated by the software applying stochastic method were used for the
 188 dynamic modeling of the water requirements and the photovoltaic pumping system.

189

190 **Table 1: Climatic data for Xining.**

191 **3.2 Water demand**

192 The model adopted for the estimation of the water demand was based on assumptions regarding the crop and
 193 soil characteristics. In this study Alfalfa was chosen as growing crop whereas the characteristics of the ground
 194 referred to a sandy soil. Both characteristic parameters of the growing crop and soil used in this model and
 195 equations for the assessment of both average daily water requirements were taken from guidelines provided by
 196 FAO [5]. The reference evapotranspiration was estimated through the method FAO Penman-Monteith that is a
 197 procedure based on the climatic data of the site chosen for the irrigation system.

198 The daily trend of the reference evapotranspiration ET_0 was calculated taking into account the monthly average
 199 daily climatic data regarding solar radiation, temperature, humidity, vapor pressure and wind speed through the
 200 following equation:

$$201 \quad ET_0 = \frac{0.408 \Delta (R_n - G) + \gamma \frac{900}{T + 273} u_2 (e_s - e_a)}{\Delta + \gamma (1 + 0.34 u_2)} \quad (1)$$

202 Where, Δ is the slope of the vapour pressure curve, R_n is the daily net radiation at the crop surface, G is the soil
 203 heat flux density, γ is the psychrometric constant, e_s is the saturation vapor pressure, e_a is the average daily actual
 204 vapor pressure and u_2 is the average monthly daily wind speed. The net radiation can be estimated as difference
 205 between the incoming net shortwave radiation and the net outgoing longwave radiation. Based on the hourly

206 data of the involved parameters, the hourly water demand can be calculated from Equation 1 adjusted for one
207 hour time step.

208 The evapotranspiration in standard cultural conditions, ET_c , was estimated from the reference value on the
209 basis of the growing crop, climatic conditions, and soil characteristic parameters and the vegetative phase. These
210 previous considerations are summed up in the cultural coefficient K_c . Then, ET_c is given by:

$$211 \quad ET_c = K_c ET_0 \quad (2)$$

212 In the specific case of Alfalfa K_c varies from 0.4 to 0.95 depending on the growing phase of the crop: K_c equal to
213 0.4 in development phase, 0.95 during the intermediate phase and 0.9 in the final phase. The development phase
214 runs from the sowing to the effective full ground cover, the intermediate stage from the effective full cover up to
215 the crop ageing and the final stage from the ageing up to the harvesting. In order to size the system, in this study
216 K_c was assumed equal to 0.95. The daily gross water volume needed by the crop W_g in mm/day can be estimated
217 taking into account evapotranspiration in the standard cultural conditions, effective rainfall, potential application
218 efficiency (PAE) and leaching requirement (LR). The gross water volume in mm/day is given by the following
219 equation:

$$220 \quad W_g = \frac{ET_c - P_e}{(1 - LR) \left(\frac{PAE}{100} \right)} \quad (3)$$

221 where P_e is the effective rainfall, which was estimated from the monthly precipitation data by applying the Soil
222 Conservation Service (SCS) method developed by the United States Department of Agriculture [16]. In this
223 equation, LR implies the amount of water needed in order to remove residual salts from the root zone whereas
224 PAE refers to the efficiency of the irrigation plant. LR and PAE were set equal to 0.18 and 0.8 correspondingly,
225 when assuming to use a micro irrigation system.

226 Another important parameter for PVWPS is the irrigation turn that permits the planning of the irrigation. The
227 irrigation turn was estimated as the ratio between the amount of water released during an irrigation turn, W_t , and
228 the daily gross water volume. W_t represents the maximum water volume that the crop can absorb without water
229 losses. It depends on the water fraction absorbed by the crop, the wet surface due to the irrigation system, the
230 roots depth and the soil water content [17].

231 The sizing of the system was based on the monthly average daily water demand, whereas the dynamic
232 modeling was based on hourly values. The estimated hourly water demand was then compared with the hourly
233 water supplied by the PV pumping system. Comparisons between water demand and water supply were made
234 also considering a time step equal to the irrigation turn and on monthly basis for the whole season.

3.3 Photovoltaic array

The power output provided by the PV array varies especially due to the different conditions of solar radiation and temperature. Indeed those previous parameters affect the characteristic curve of the PV modules. The dynamic modeling of the PV system considered the estimation of the hourly power output of the solar array $P(T, \vartheta)$, depending on the hourly beam radiation I_b and diffuse radiation I_d , incidence angle ϑ and temperature T . The following equation was used to evaluate the hourly power output from 1 kW_p PV array [18]:

$$P(T, \theta) = [\eta_{0b} K_b(\theta) I_b + \eta_{0d} K_d I_d] [1 + (T_c - T_r) \alpha] \quad (4)$$

Where η_{0b} is the optical efficiency for the beam radiation, $K_b(\vartheta)$ is the incidence angle modifier, K_d is the incidence modifier for diffuse radiation T_c is the cell temperature, T_r is the reference temperature (25°C) and α is the power temperature coefficient. The first term of Equation 4 represents the power output from 1 kW_p PV modules at the reference temperature, whilst the second term accounts for the power losses due to temperature deviation from the reference value. The influence of the temperature on the PV modules performance was taken into account through the cell temperature T_c that is affected by the ambient temperature T_a and the global solar radiation I_{tot} through the following equation:

$$T_c = T_a + \left[\frac{(NOCT - 20)}{800} \right] I_{tot} \quad (5)$$

Where, $NOCT$ is the nominal operating cell temperature. Simulations of the power output from the PV array were conducted with WINSUN that is software based on TRNSYS system simulation [9]. The dynamic modeling of the solar array power output was estimated taking into account the hourly values of beam radiation, diffuse radiation, incidence angle and ambient temperature. The calculations carried out with WINSUN considered the effects of both optical efficiencies and angle modifiers, whereas the effect of the temperature was estimated separately through a MATLAB script. Both fixed array and fully tracking array were investigated in this work. The sizing of the PV water pumping system was carried out through a simple approach based on the daily hydraulic energy E_h required to lift the water demand, the average daily radiation on the plane of the array $I_{tot,d}$ and the overall system efficiency η_s . This approach is summed up in the following equation [19]:

$$P_{peak} = \frac{E_h}{I_{tot,d} \eta_s} \quad (6)$$

The daily hydraulic energy was estimated from the daily water demand and hydraulic head with the following formula:

$$E_h = \rho g H W_g \quad (7)$$

263 Where ρ is the water density and g is the gravity acceleration. In Equation 7 W_g is expressed in m^3/ha day (1
 264 mm/day corresponds to $10 m^3/ha$ day). The efficiency of the system takes into account the efficiency of the MPPT
 265 system, controller or inverter, electric engine, centrifugal pump and system losses [20, 21].

266 3.4 DC/DC converter-motor-pump

267 The model used in this work for the converter and inverter was based on the assumption that the output power
 268 is equal to the input power from the photovoltaic generator less the unavoidable power losses associated.
 269 Normally the efficiency varies between the 80% up to the 95 % depending on working conditions, especially
 270 temperature, and power available. The power losses were taken into account on the basis of an average
 271 efficiency of the power controlling system.

272 The motor-pump was sized on the basis of instantaneous water flow, estimated from daily water demand and
 273 daily operating hours, and hydraulic discharge. The total dynamic head was calculated taking into account several
 274 contributions such as outlet minimum pressure required by the irrigation system, height of the of the outlet pipe
 275 above the ground surface, depth of the static water level, depth of the dynamic water level and friction losses due
 276 to the pipeline circuit. In this study a hydraulic discharge measured in field tests was used. The sizing of the
 277 centrifugal motor-pump in kW was carried out with the following equation:

$$278 P = \frac{\rho g Q H}{1000 \eta_p} \quad (8)$$

279 Where, Q is the flow expressed in m^3/s , 1000 is a conversion factor and η_p is the efficiency of the motor pump
 280 system.

281 The motor-pump system was modeled on the basis of the governing equations of the electric engines, affinity
 282 laws and hydraulic power. The main input data regarding the minimum and maximum head and the
 283 corresponding flows and efficiencies, were taken from motor-pump datasheet provided by pumps manufacturer
 284 companies [22, 23]. The dynamic modeling of the pump was carried out considering the pump characteristic
 285 curve that expresses the instantaneous water flow in m^3/h versus the hourly feeding power to the motor-pump
 286 system. A typical expression of the relationship between water flow Q , hydraulic discharge H and power input P_{in}
 287 is given by the following third grade polynomial:

$$288 Q(H, P_{in}) = c_1(H)P_{in}^3 + c_2(H)P_{in}^2 + c_3(H)P_{in} + c_4(H) \quad (9)$$

289 Where, c_1 , c_2 , c_3 and c_4 are experimental coefficients. The previous curves, both for the DC and AC pump, were
 290 obtained from PVsyst (v5.55) through the specific tool for pumping system and adjusted with the curve fitting
 291 function in MATLAB.

4. RESULTS AND DISCUSSIONS

This section shows the results regarding the assessment of water demand and solar energy, sizing and modeling of the system, matching between water demand and water supply and economics analysis between DC and AC pump and fixed and fully tracking PV array. In this work an irrigated area of 1 ha was considered.

4.1 Assessment of the water demand

The monthly average water demand for the growing of Alfalfa on a sandy soil and the trend of the monthly average precipitation are presented in Figure 3.

Figure 3: Monthly average daily water demand.

It is clear that the trend of the daily water demand for irrigation is affected mainly by the evaporation related to the growing phase and rainfall. The evapotranspiration registered a peak during the sunniest months of the year whereas the precipitation registered the highest values in the period May-September. The irrigation season for the crop chosen is five months, this study interested then only the months from May to September. In this work it was assumed that in May takes place the development phase, in June and July the intermediate phase and in August and September the final phase. The Alfalfa water demand trend shows then a peak during the month of June of $47 \text{ m}^3/\text{ha}$ and it decreases during the remaining months. The minimum daily water demand estimated for this period corresponded to the water requirements in May which is equal to $10.4 \text{ m}^3/\text{ha}$. The irrigation turn estimated by the model was 10 days. In this work an irrigated area of 1 ha was considered. The validation of the results obtained from the water demand model was carried out through personal communication with field expert and with the results obtained in field studies conducted in the same region [24]. The former proved that the daily maximum water requirement for irrigation is $50 \text{ m}^3/\text{ha}$. Whereas the results obtained in previous field studies showed an irrigation duty of $600 \text{ m}^3/\text{ha}$ for an irrigation turn of 14 days corresponding to $40 \text{ m}^3/\text{ha}$ day.

4.2 Solar energy assessment

The available solar radiation and its variation with the tilt angle and system technology are shown in Figure 4. In this study it was assumed to use a fixed system with an azimuth angle equal to 0° that corresponds to solar array oriented towards south. The results of the simulations show that for the fixed system the best tilt angle on annual basis was 30° with a corresponding collectable solar radiation of 1870 kWh/m^2 year. For the simulations carried out only during the irrigation season, from May to September, the best tilt angle resulted in 10° collecting 854 kWh/m^2 season. The 10° tilted solar array was then used in our study. As regards the fully tracking system, the annual collected solar radiation on the plane surface was 2490 kWh/m^2 year whereas 1120 kWh/m^2 during the irrigation season. This corresponds to a collected solar energy 30 % higher compared to the optimal fixed system.

Figure 4: Solar energy available depending on the tilt angle and system technology.

326 The power output from fixed and fully tracking PV system with a capacity of 1 kW_p during a sunny day in June is
327 shown in Figure 5. The energy collected by the 10° tilted system was 7.0 kWh/m² whereas the solar energy
328 collected by the fully tracking array it was equal to 10 kWh/m² corresponding to 40% more energy than the fixed
329 system. The better performances of the sun fully tracking system are mainly due to the system, varying
330 continuously its tilt and azimuth angle in order to follow the sun, optimizes the harnessing of available solar
331 radiation guaranteeing a wider range of working hours at higher power output compared to the fixed system.

332

333
334

Figure 5: 1 Kw_p power output during a sunny day in June.

335 It is clear that the solar generator power output depends on the variation of the available solar power and is
336 mainly sensitive to the variation of ambient temperatures. The typical effect of the hourly variation of ambient
337 temperature on the power output of solar array is presented in Figure 6 for 1 kW_p PV array.

338

339

Figure 6: Effect of the temperature on the power output of 1 kW_p solar array.

340

341 The power output from the solar generator without considering the temperature effect, is the power at the
342 reference temperature of 25 °C and depends only on the available solar radiation, PV modules optical efficiency
343 and incidence angle modifiers. As it is shown, the temperature affects the power generation of the solar array
344 during the sunniest and warmest hours of the day due to the difference between cell temperature and reference
345 temperature. The maximum drop of the efficiency and the subsequent drop of power generation were registered
346 at 1 pm and it was equal to 198 W representing a loss of 17 %. The high value of power waste was due to the
347 theoretical approach used in this study to perform the effect of temperature on the PV modules efficiency. The
348 previous approach tends to overestimate the power losses due to temperature, usually in the range of 10 %, on
349 behalf of guaranteeing more accurate water supply forecasts.

350 **4.3 Pump modeling**

351 The sized PV systems were used in dynamic simulations in order to estimate the hourly power output and hourly
352 water pumped. The dynamic modeling of the photovoltaic pumping system could further verify if the sized system
353 could fulfill the dynamic water requirements. The water pumped under different PV power output was estimated
354 on the basis of the pump characteristic curve flow rate against power input. Obviously, the instantaneous
355 pumped water flow is mainly affected by the variation of the power coming from the solar array. Figure 7 shows
356 the instantaneous water flow at different motor power input.

357

358

Figure 7: Instantaneous water flow compared to the power input to the motor.

359

360 In the case of the AC technology the engine starts to drive the pump when is reached a minimum feeding power
 361 of 0.37 kW. The instantaneous flow increases with the input power until reaching 1.5 kW. The motor-pump speed
 362 is governed in the above mentioned power range following the pattern outlined. For input power greater than 1.5
 363 kW the speed and then the water output was kept constant and equal to the maximum due to the power
 364 conditioning system interface in order to avoid damages to the electric engine. In the case of the DC motor the
 365 power working range varies from 0.15 kW and 1.6 kW.

366 4.4 Sizing of the system

367 The sizing of PV array and pump was then made on the basis of the water demand, total dynamic head, solar
 368 energy available and efficiencies of the system. The system was sized on the basis of the worst month marked out
 369 by the lowest ratio between monthly daily average solar radiation and monthly daily average water demand, as
 370 shown in Table 2.

372 **Table 2: Solar energy and water demand ratio.**

373
 374 June presented the lowest ratio between daily solar radiation and water demand especially due to the highest
 375 water requirements registered during the irrigation period. June was then chosen as designing month. According
 376 to the estimation of water demand, 47.1 m³ of water is needed every day during the irrigation turn. The PV array
 377 peak power was estimated on the basis of the daily hydraulic energy required to achieve a hydraulic head of 40 m
 378 and the monthly average daily solar radiation. The resulting required hydraulic energy was 5 kWh/day whereas
 379 the resulting monthly average daily solar radiations were 6.0 kWh/m² and 7.8 kWh/m² for fixed system and fully
 380 tracking system respectively. The sizing procedure for the PV array peak power is also affected by the efficiencies
 381 of controller or inverter, electric engine, pump and other unavoidable system losses due mainly to power losses
 382 of PV modules affected by temperature variation and electric losses in the wires. All these contribution are
 383 summarized in the overall system efficiency η_s given by the following:

$$384 \quad \eta_s = \eta_{pc} \eta_p \eta_{PV,T} \eta_w \quad (10)$$

385 Where η_{pc} is the efficiency of the power conditioning system, η_p is the efficiency of the pumping system and $\eta_{PV,T}$
 386 and η_w consider the losses power losses in the PV modules and wires. These efficiencies vary with device models
 387 and working conditions. For example, the efficiency of the power conditioning system is affected mainly by the
 388 power input and ambient temperature varying between 80 % and 95 %, the motor pump efficiency varies from 40
 389 % up to 60 % depending on power input, water flow and pressure. In this study, in order to take into account the
 390 effect of components efficiency on the system performances, three values of the system efficiency were tested in
 391 the design and subsequently proved through dynamic simulations: 30%, 35% and 40% respectively. This resulted
 392 in three different PV array sizes for both fixed and fully tracking installation. The resulting PV array power were
 393 2.8 kW_p, 2.4 kW_p and 2.1 kW_p for the fixed system and 2.1 kW_p, 1.8 kW_p and 1.6 kW_p for the two-axes tracking

394 system respectively. On the basis of the power peak obtained, the corresponding PV area was estimated
395 assuming an energy conversion efficiency of the PV panels equal to 14.3 % [25]. The pump capacity was estimated
396 according to the hydraulic head and the instantaneous water flow. The instantaneous water flow was estimated
397 from the daily water demand assuming 8.5 operating hours. The required pump power resulted in 1.5 kW.
398 According to the pumps available on the market, the following pumps were adopted: 1.6 kW DC centrifugal
399 multistage and 1.5 kW AC single phase centrifugal multistage. The main input data and results of the designing
400 phase are summarized in Table 3.

401
402 **Table 3: Summary of the main system parameters and sizing results.**

403
404 **4.5 Design proving**

405 Concerning the worst situation in June, the simulated pumped water was compared with the estimated daily
406 water demand in order to identify the mismatches. The simulation step was set equal to the irrigation turn, 10
407 days, period marked out by a water demand of 470 m³.

408 As the motor-pump system was driven by a 2.8, 2.4 and 2.1 kW_p fixed PV arrays, the pumped water during the
409 first irrigation turn in June amounted to 515, 470 and 426 m³ respectively when using the DC pump; while 599,
410 531 and 470 m³ respectively when using the AC pump. Therefore, the system of AC pump can always satisfy the
411 water demand. However, for the system of DC pump centrifugal pump, it has to be driven by a PV array larger
412 than 2.4 kW_p in order to achieve the pumped water could match the water demand. For the case of DC
413 centrifugal pump driven by 2.1 kW_p PV array the mismatch was 44 m³. The achieved results through dynamic
414 simulations for the fixed PV systems are presented in Figure 8.

415
416 **Figure 8: Pumped water flow during an irrigation turn in June with fixed PV array.**

417
418 As the solar arrays mounted on the two-axis tracking system, the amounts of pumped water in June were
419 calculated as 546, 492 and 448 m³ for the 2.1, 1.8 and 1.6 kW_p respectively when using DC pump; while 634, 553
420 and 486 m³ respectively when using AC pump. It is similar the situation of fixed PV system that the system of AC
421 pump can always satisfy the water demand. For the system of DC pump, the PV array has to be larger than 1.8
422 kW_p. The better performances of the AC pump compared with the DC were mainly due to the specific
423 characteristic curve power input against instantaneous water flow. Although the DC pump is marked out by a less
424 required power input to start running the pump and a higher rated power compared to the AC pump, the latter is
425 featured by a higher water flow output for input power greater than 0.7 kW resulting in greater volume of water
426 pumped. The dynamic simulations results for the sun tracking PV systems are presented in Figure 9.

427
428 **Figure 9: Pumped water flow during an irrigation turn in June with tracking PV array.**

429

430 It is clear that the overall efficiency used in the sizing phase affected the amount of pumped water. The
431 achieved results show that a suitable design of the DC pumping system driven by the fixed PV array is based on
432 overall efficiency of both 30% and 35%. These efficiencies permitted during the dynamic simulation to achieve the
433 amount of water needed for the irrigation purposes. Efficiency equal to 35 % permitted to both fulfill the water
434 requirements and minimize the PV modules area optimizing the system. Even in the case of DC pumping system
435 driven by the fully tracking PV array, both 30% and 35% were suitable efficiencies for the designing of the system.
436 In the case of the AC pump powered by the fixed solar array, the optimization of the system was achieved by an
437 efficiency of 40 % considered during the design process both for the fixed and fully tracking PV array. It has to be
438 pointed out that it doesn't imply that the high system efficiency is not desirable. The reason that the high
439 efficiency system (40%) has a worse performance is mainly due to that the efficiency considered in the design
440 stage is based on steady performance. However, in order to represent the dynamic characters of both the
441 climatic conditions and the system components, dynamic efficiencies may be required. Therefore, it is of great
442 importance to conduct the dynamic simulation to prove the design and find the optimal value. Meanwhile, the
443 overall system that accounts for the components dynamic efficiencies and, as the achieved results show, the
444 optimal value can be set only through dynamic simulations need to be included in the future study to have a more
445 accurate simulation.

446 The water output simulations were extended to the whole irrigation season as well, from May to September,
447 comparing the crop variable water demand depending on the growing phase with the variable water supply due
448 to the variation of available solar energy. Both DC and AC pump technology and optimal fixed and sun tracking
449 array were used in these simulations. The monthly results about water demand and water supply are shown in
450 Figure 10. Since that the water pumping system was sized for the worst month, there was then a surplus of
451 pumped water during the months featured by a higher solar energy and water demand ratio than the
452 corresponding designing month. Indeed, the water demand for Alfalfa varies during the irrigation season
453 depending on the crop growing period. Simultaneously the available solar radiation varies during the irrigation
454 season affecting the power output and then the pumped water.

455

456 **Figure 10: Monthly water demand and supply estimated through dynamic simulations.**

457

458 Moreover, when extending the simulations to one month instead of within one irrigation turn (ten days), some
459 critical situations occur. It is clear from Figure 10 that both DC and AC driven by tracking PV array could fulfill the
460 water requirements in June. However, when fixed PV array is used, some mismatching between water supply and
461 water demand were identified: 13 m³ for the DC pump system driven by 2.4 kW_p PV array and 24 m³ for the AC
462 pump system driven by the 2.1 kW_p PV array. The mismatching identified in the monthly simulation was the result
463 of the dynamic variability of solar radiation affecting the water output from the pumping systems. As shown in

464 Figure 11, days marked out by poor solar energy conditions can considerably affect the amount of pumped water
465 but without substantially affecting the water demand since the latter depends on more climatic parameters, such
466 as humidity, wind and rainfall. Moreover, in periods or months marked out by lower solar energy, such as
467 September, systems using DC pump technology offered better performances in terms of water supply due to the
468 lower power input requirements.

469 The surplus of pumped water recorded during the irrigation season could be used in order to extend the
470 irrigated area or for other purposes in order to use the system more effectively. For example, if the surplus of
471 water is used for irrigation, for the AC pump system driven by the 1.6 kW_p PV tracking array, the irrigated area can
472 be extended up to 4.9 ha when it is in May and 1.7 ha in August and September; while for the DC pump system
473 driven by 1.8 kW_p PV tracking array, the irrigated area can be extended to 4.7 ha in May and 1.7 and 1.8 in August
474 and September respectively.

475

476 **Figure 11: Hourly dynamic simulations of water demand and water supply from AC pump powered by 2.1 kW_p solar**
477 **array.**

478

479 **4.6 Economic analysis**

480 An economic analysis based on the investment costs was carried out in order to investigate the most cost
481 effective solution among the alternatives presented in this study especially between system equipped with fixed
482 and sun tracker array and AC and DC pump technology. This analysis was performed in order to combine both
483 economic aspects and performances in terms of water pumped according to the crop water requirements
484 previously discussed.

485 The prices of the PV modules are highly variable depending on the market and the manufacturer company.
486 Nevertheless it represents one of the major costs for a photovoltaic pumping system, accounting for more than
487 the 30 % of the overall costs (considering in the economic analysis the cost of well digging). Using the sun tracking
488 system permits a smaller area of PV modules which resulted in a deducted capital cost of PV cells and power
489 conditioning system. But at the same time the tracker can highly contribute on the overall cost of the system
490 mainly due to its high accuracy technology. Moreover, DC pump are more expensive compared to AC pump but
491 on the contrary the controller used as interface between the PV modules and the DC electric engine is more
492 affordable than DC/AC inverter. Comparing the 1.8 kW_p two-axis tracking system with the 2.4 kW_p fixed solar
493 array powering the DC pumping system, although the tracking system has a power peak about 30% less than the
494 fixed system, the former offers better performances than the latter due to the daily higher exploitability of solar
495 energy. The AC pump driven by the fixed 2.1 kW_p PV array fulfilled the water requirements as the DC pump
496 powered by the fixed 2.4 kW_p solar generator saving 0.3 kW_p of solar cells. Even the AC pumping system powered
497 by the 1.6 kW_p solar generator mounted on the tracking system fulfilled the water requirements avoiding the

498 installation of 0.8 kW_p of solar cells compared to the DC 2.4 kW_p fixed system and 0.5 kW_p of PV modules
499 compared to the AC 2.1 kW_p fixed system.

500 The PVWPS systems compared in terms of initial investment costs (IIC) in this economic analysis were the same
501 systems compared in terms of water pumped in the previous section of this paper. The possibility to install
502 tracking system instead of fixed system and DC instead of AC pump was estimated. All the prices used in the
503 investigation, summarized in Table 4, were taken from a business-to-business online platform and refer to the
504 Chinese market [16].

505

506

Table 4: PV water pumping system components unit costs.

507

508

509 The results of the economic analysis are presented in Figure 12, outlining the total initial capital cost together
510 with the costs contributions.

511

512

Figure 12: Total initial investment costs for the PVWPS proposed.

513

514 On the basis of the economic investigation carried out, the most cost effective solution was the AC 2.1 kW_p
515 fixed system with an overall initial capital cost of 2450 \$ followed by the DC 2.4 kW_p system marked out by an
516 initial capital cost of 2950 \$. The reason that the DC fixed system has a higher investment compared with the
517 corresponding AC fixed system was mainly due to the cost difference of DC and AC pump, 640 \$ against 150 \$,
518 rather than the cost difference of PV modules, 1440 \$ against 1260 \$. Despite of the reduction in cost due to the
519 installation of DC/DC converter on behalf of the installation of DC/AC inverter, the AC fixed system was the most
520 cost-effective solution. Comparing the fixed system with the corresponding systems equipped with the sun
521 tracker device, the formers presented lower investment cost than the latter especially because of the high
522 investment cost due to the tracking system. The tracked DC 1.8 kW_p system had an investment cost of 4350 \$ of
523 which 1620 \$ were due to the sun tracking device accounting for 37 % of the overall cost. The cost reduction due
524 to the lower investment in PV modules and power conditioning system using sun tracking technology had no
525 positive effects. A possible application of PVWPS equipped with solar tracker could be economically supported in
526 the case the system is used for multipurpose applications during the months where the irrigation is not needed.

527 5. CONCLUSIONS

528 In this study a dynamic simulation tool combining the models of the water demand, the solar PV power and
529 pumping system was developed in order to be used for quick design and design validation. According to the
530 achieved results the following conclusion can be pointed out:

- 531 • The sizing of photovoltaic water pumping systems for irrigation is extremely affected by the dynamic
532 character of the water demand and collectable solar energy. In order to define the worst condition on

533 the basis of which the system is sized, the lowest ratio between required hydraulic energy and available
534 solar radiation has to be considered.

- 535 • The assessment of the overall system efficiency η_s is relevant to optimally size the PV array power peak
536 avoiding both system failure and economic losses. η_s summarizes in a steady value the dynamic
537 efficiency of the system components and the optimal value can only be set through system dynamic
538 simulations verifying the match between pumped water and water demand.
- 539 • Preliminary economic analysis based on the initial investment costs showed that AC pump powered by
540 fixed PV array represent the most cost-effective solution for water pumping.

541 **ACKNOWLEDGEMENTS**

542 The authors are grateful to the Swedish International Development Cooperation Agency (Project No.: AKT-2010-
543 040) for the financial support.

544 **REFERENCES**

- 545 [1] Argaw N, Foster R, Ellis A. Renewable Energy for Water Pumping applications in rural villages. NREL. 2001.
- 546 [2] IEA, Policy recommendations to improve the sustainability of rural water supply systems. Report IEA-PVPS T9-
547 1:2011.
- 548 [3] IEA, 16 Case studies on the deployment of photovoltaic technologies in developing countries. Report IEA-PVPS
549 T9-07:2003.
- 550 [4] IEA, Trends in photovoltaic applications survey report of selected IEA countries between 1992 and 2010,
551 Report IEA-PVPS T1-20:2011.
- 552 [5] Allen RG, Pereira LS, Raes D, Smith M. Crop evapotranspiration. Guidelines for computing crop water
553 requirements. FAO. 1998.
- 554 [6] Bouzidi B, Haddadi M, Belmokhtar O. Assessment of a photovoltaic pumping system in the areas of the
555 Algerian Sahara. Renewable & Sustainable Energy Reviews 2008. 13: 879-886.
- 556 [7] Meteonorm, <http://meteonorm.com/>, 2012-01-30.
- 557 [8] Perers B, Karlsson B. Energy and building design. Lund University, Faculty of Engineering (LTH); 2007. WINSUN
558 Based on TRNSYS/TRNSED/PRESIM 14.2.
- 559 [9] Castaner L, Silvestre S. Modelling photovoltaic systems using PSpice®. 1st ed. UK: Wiley. 2002.
- 560 [10] Hsiao YR. Direct coupling of photovoltaic power source to water pumping system. Solar Energy 1983. 32(4):
561 489-498.
- 562 [11] Hamidat A, Benyoucef B. Systematic procedures for sizing photovoltaic pumping system using water tank
563 storage. Energy Policy 2009. 37: 1489-1501.
- 564 [12] Bakelli Y, Arab AH, Azoui B. Optimal sizing of photovoltaic pumping system with water tank storage using
565 LPSP concept. Solar Energy 2011. 85:288-294.

- 566 [13] Ould-Amrouche S, Rekioua D, Hamidat A. Modelling photovoltaic water pumping system and evaluation of
567 their CO₂ emissions mitigation potential. Applied Energy 2010. 87: 3451-3459.
- 568 [14] Fedrizzi MC, Ribeiro FS, Zilles R. Lessons from field experiences with photovoltaic pumping systems in
569 traditional communities. Energy for Sustainable Development 2009. 13: 64-70.
- 570 [15] Alibaba, <http://www.alibaba.com/>, 2012-08-30
- 571 [16] United States Department of Agriculture, Natural Resources Conservation Service,
572 <http://www.nrcs.usda.gov/wps/portal/nrcs/main/national/home>, 2012-02-01.
- 573 [17] A. Capra, B. Scicolone, "Project and management of irrigation plant-Criteria for the use and exploitation of
574 water for irrigation purpose". 2007. 1st ed. Edagricole. (In Italian)
- 575 [18] J. A. Duffie, W.A. Beckman. Solar Engineering of Thermal Processes. 3rd ed. 2006. Wiley.
- 576 [19] S. R. Wenham, M. A. Green, M. E. Watt, R. Corkish, "Applied photovoltaics", Second Edition, Earthscan
- 577 [20] Khatib T. Design of photovoltaic water pumping system at minimum cost for Palestine: a review. Journal of
578 applied sciences 2010. 10 (22): 2773-2784.
- 579 [21] Lynn PA. Electricity from sunlight. 1st ed. UK: Wiley. 2010.
- 580 [22] Lorentz, <http://www.lorentz.de/>, 2012-01-30.
- 581 [23] Matra, <http://www.matra.it/>, 2012-01-30.
- 582 [24] Final report. ADB RSC-C91300 (PRC). Qinghai Pasture Conservation Using Solar Photovoltaic (PV)-Driven
583 Irrigation. 2010.
- 584 [25] Schott, www.schottsolar.com/global/products/photovoltaics/schott-poly-245/, 2012-02-14

585
586
587
588
589
590
591
592
593
594
595
596
597
598
599
600

601 **Figure captions**

602 Figure 1: Schematic diagram of a photovoltaic water pumping system.

603 Figure 2: Designing and dynamic modeling procedure.

604 Figure 3: Monthly daily estimated water demand.

605 Figure 4: Solar energy available depending on the tilt angle and system technology.

606 Figure 5: 1 Kw_p power output during a sunny day in June.

607 Figure 6: Effect of the temperature on the power output of 1 kW_p solar array.

608 Figure 7: Instantaneous water flow compared to the power input to the motor.

609 Figure 8: Pumped water flow during an irrigation turn in June with fixed PV array.

610 Figure 9: Pumped water flow during an irrigation turn in June with tracking PV array.

611 Figure 10: Monthly water demand and supply estimated through dynamic simulations.

612 Figure 11: Hourly dynamic simulations of water demand and water supply from AC pump powered by 2.1 kW_p
613 solar array.

614 Figure 12: Total initial investment costs for the PVWPS proposed.

615

616

617

618

619

620

621

622

623

624

625

626

627

628

629

630

631

632

633

634

635

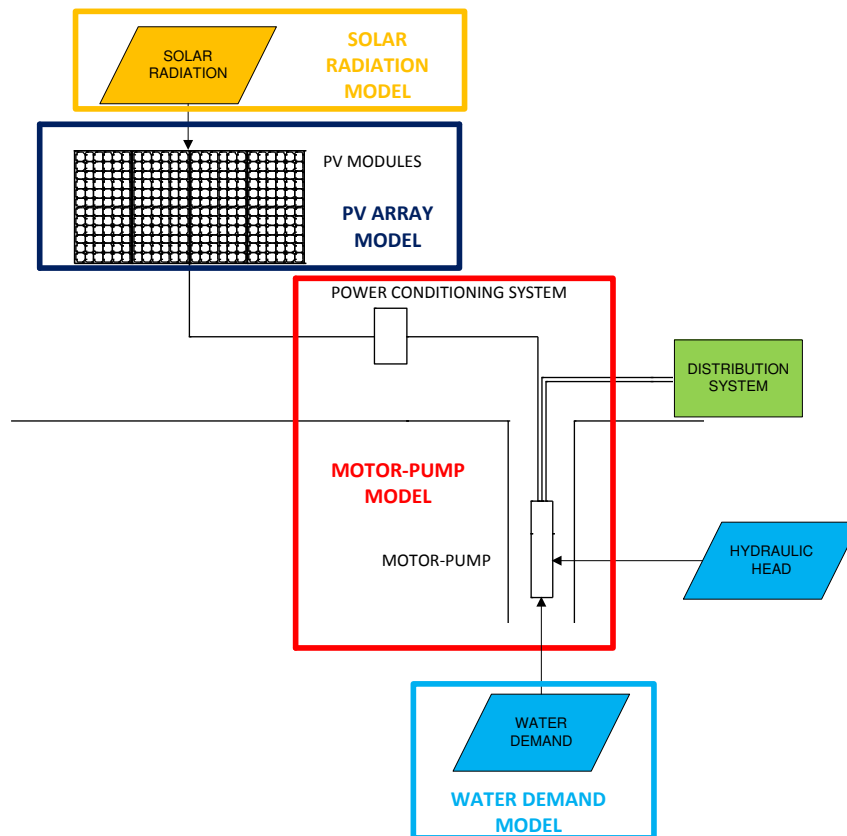


Figure 1: Schematic diagram of a photovoltaic water pumping system.

636
 637
 638
 639
 640
 641
 642
 643
 644
 645
 646
 647
 648
 649
 650
 651
 652
 653
 654
 655

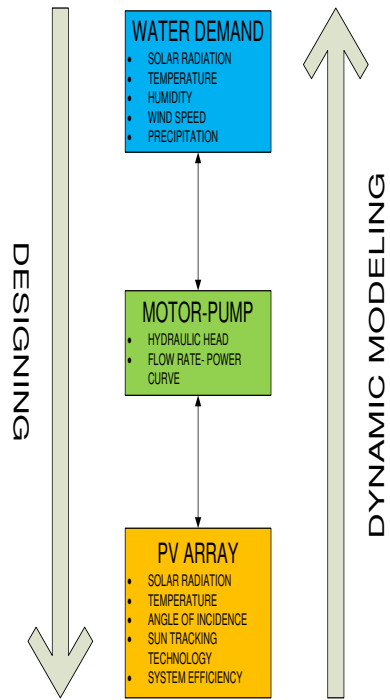


Figure 2: Designing and dynamic modeling procedure.

656
 657
 658
 659
 660
 661
 662
 663
 664
 665
 666
 667
 668
 669
 670
 671
 672
 673
 674
 675
 676
 677
 678

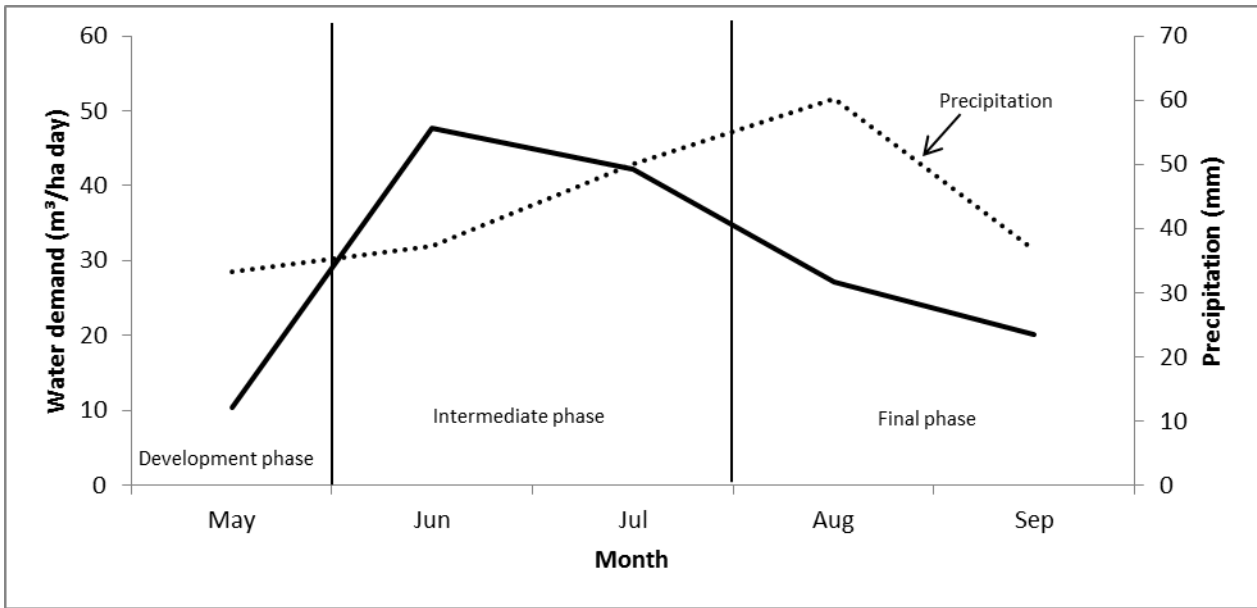


Figure 3: Monthly average daily water demand.

679
 680
 681
 682
 683
 684
 685
 686
 687
 688
 689
 690
 691
 692
 693
 694
 695
 696
 697
 698
 699
 700
 701
 702
 703
 704
 705

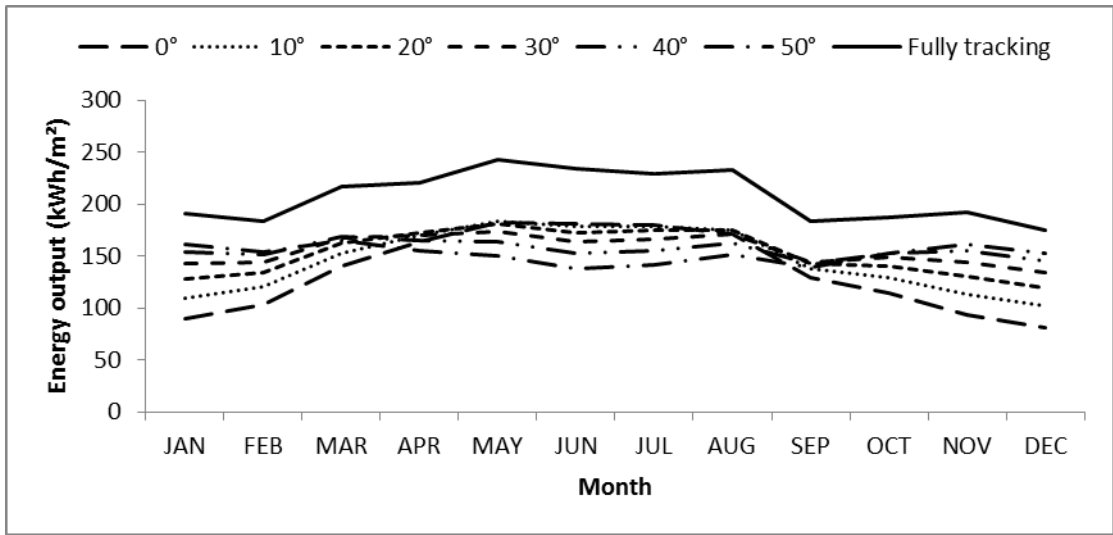


Figure 4: Solar energy available depending on the tilt angle and system technology.

706
707
708
709
710
711
712
713
714
715
716
717
718
719
720
721
722
723
724
725
726
727
728
729
730
731
732
733

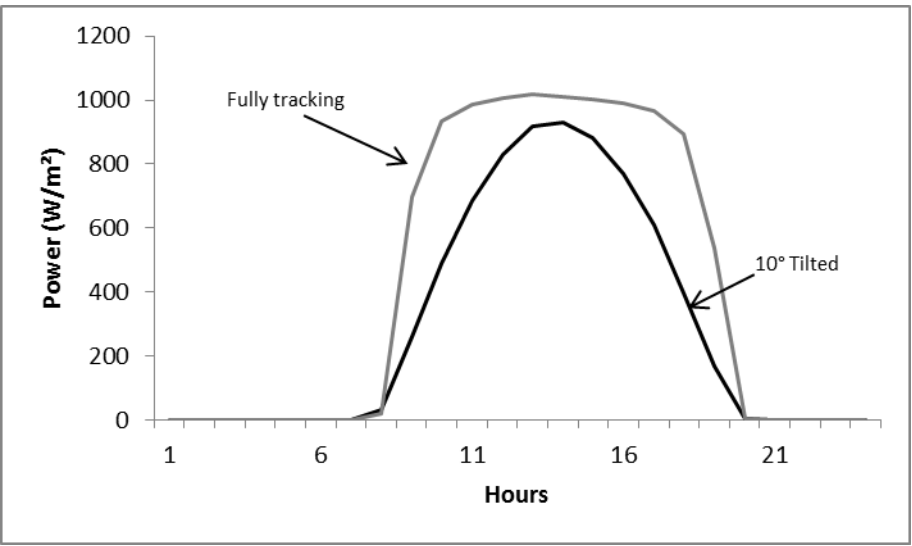


Figure 5: 1 Kw_p power output during a sunny day in June.

734
735
736
737
738
739
740
741
742
743
744
745
746
747
748
749
750
751
752
753
754
755
756
757
758
759
760
761

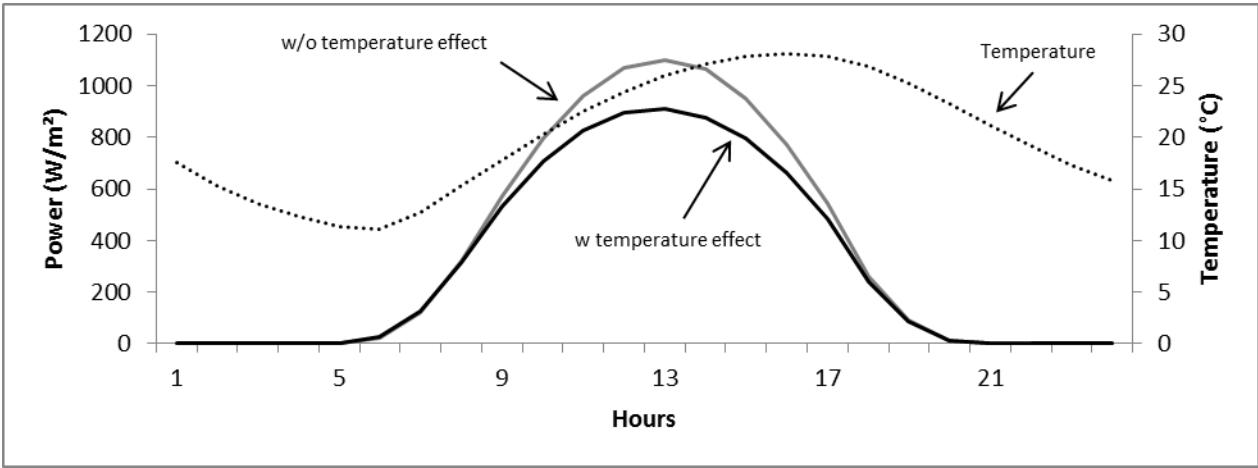


Figure 6: Effect of the temperature on the power output of 1 kW_p solar array.

763
764
765
766
767
768
769
770
771
772
773
774
775
776
777
778
779
780
781
782
783
784
785
786
787
788
789
790
791

792

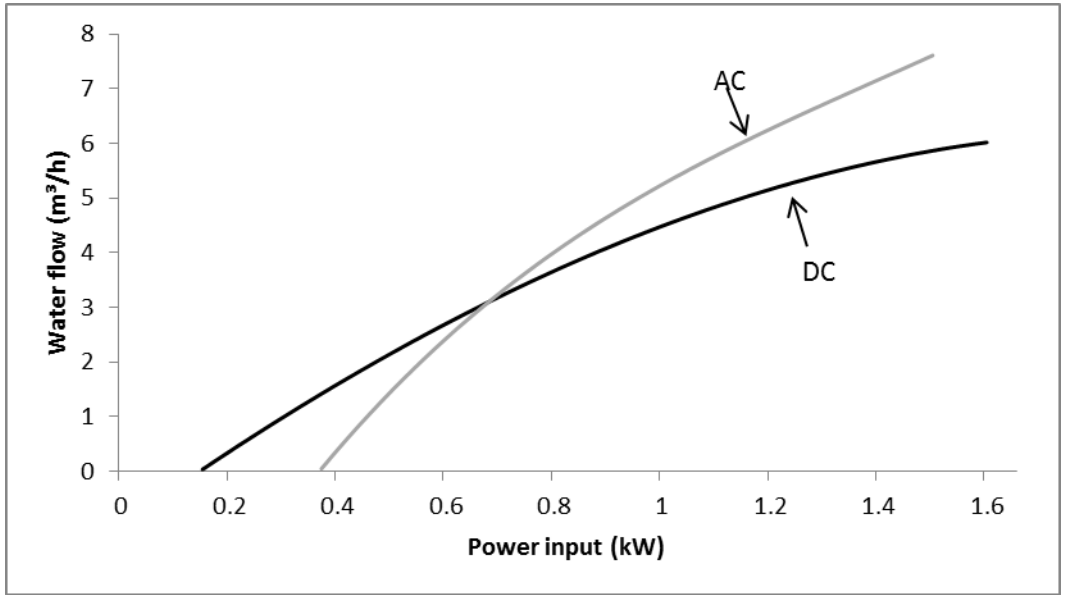


Figure 7: Instantaneous water flow compared to the power input to the motor.

793
794
795
796
797
798
799
800
801
802
803
804
805
806
807
808
809
810
811
812
813
814
815
816
817
818

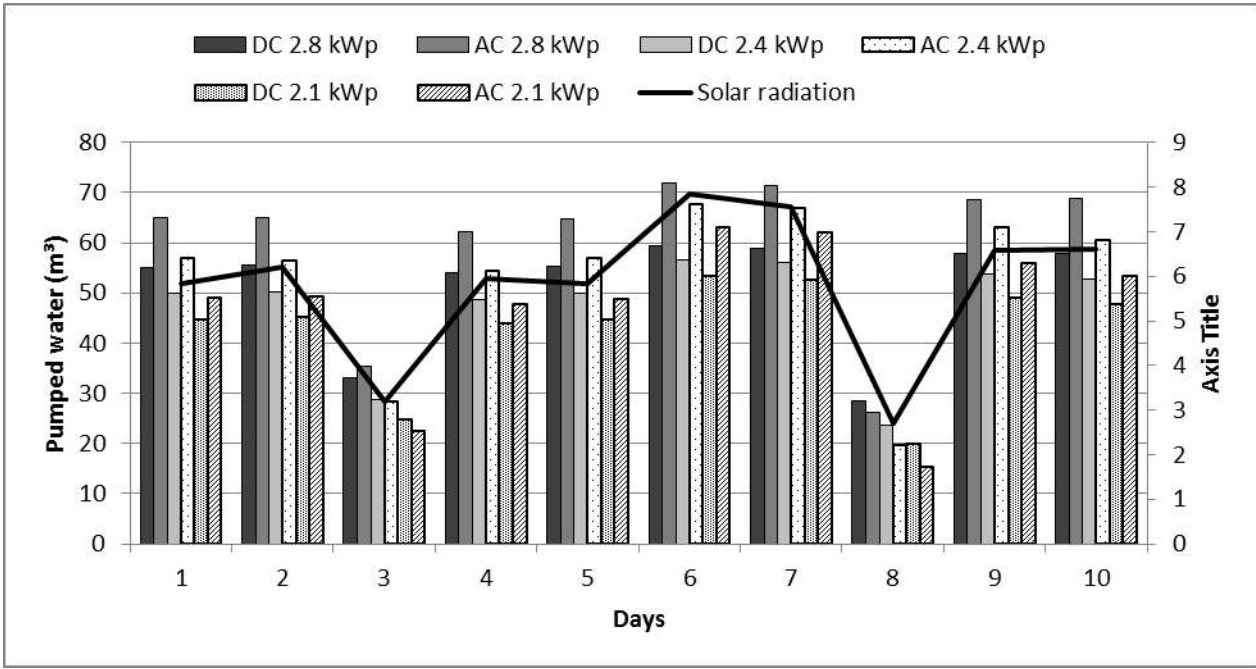


Figure 8: Pumped water flow during an irrigation turn in June with fixed PV array.

820
821
822
823
824
825
826
827
828
829
830
831
832
833
834
835
836
837
838
839
840
841
842
843
844

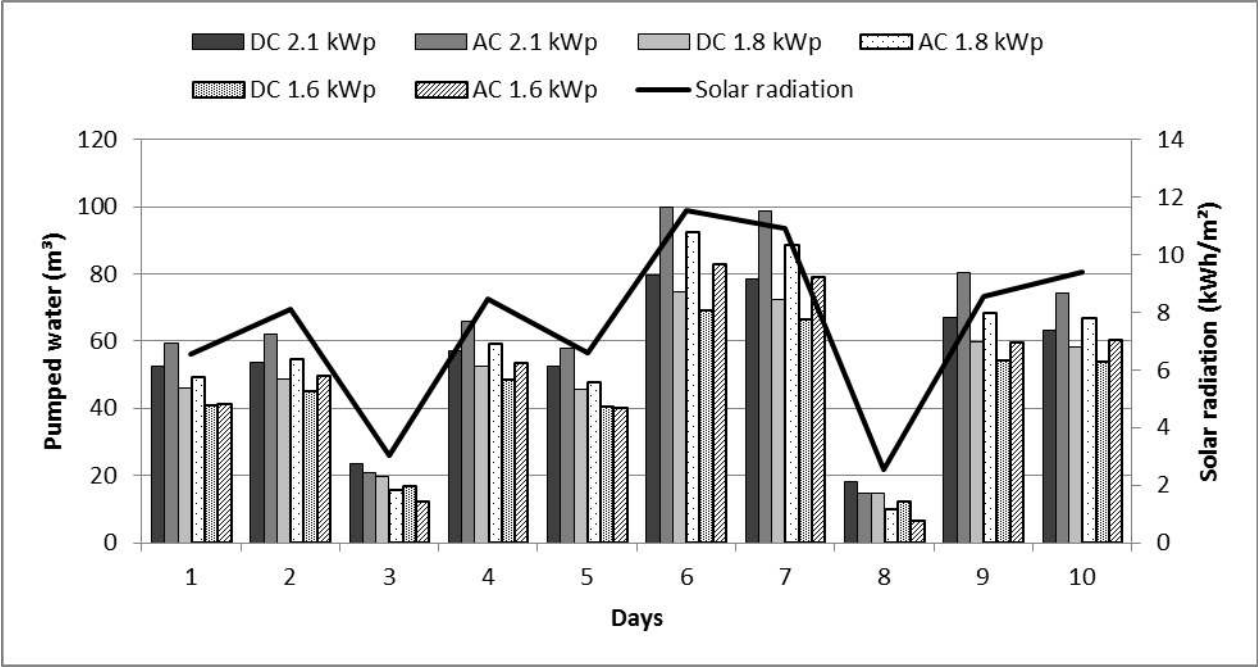


Figure 9: Pumped water flow during an irrigation turn in June with tracking PV array.

846
847
848
849
850
851
852
853
854
855
856
857
858
859
860
861
862
863
864
865
866
867
868
869
870

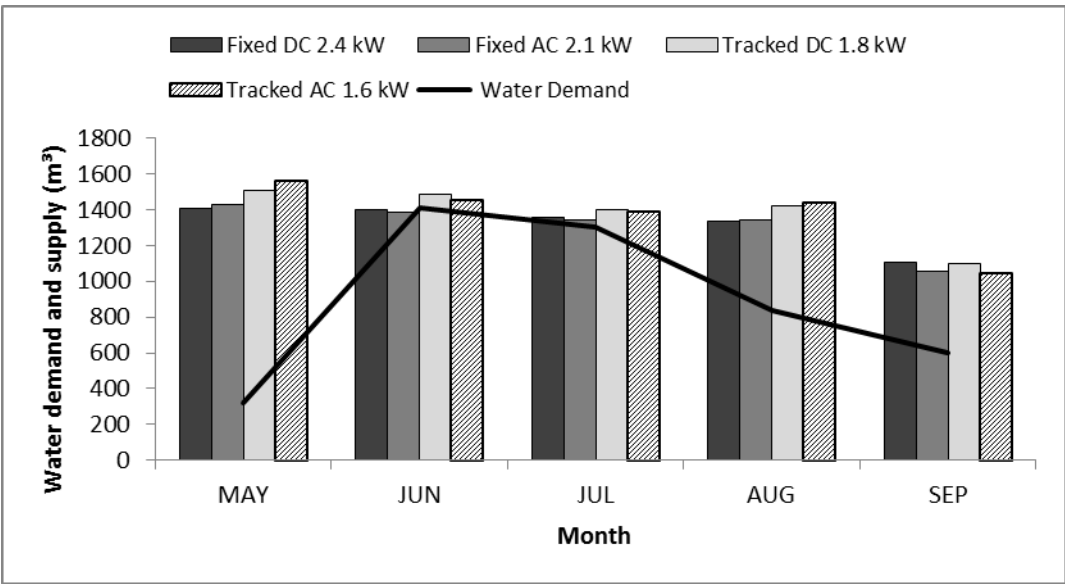
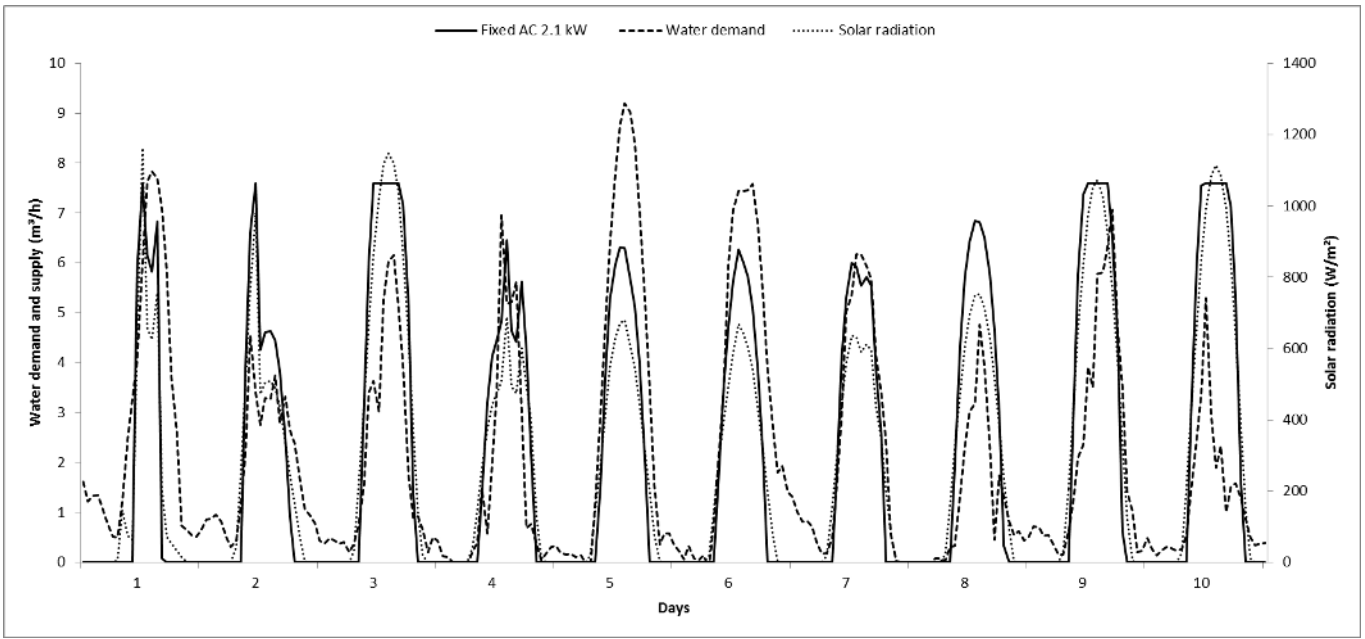


Figure 10: Monthly water demand and supply estimated through dynamic simulations.

871
 872
 873
 874
 875
 876
 877
 878
 879
 880
 881
 882
 883
 884
 885
 886
 887
 888
 889
 890
 891
 892
 893
 894
 895
 896
 897



898
 899 **Figure 11: Hourly dynamic simulations of water demand and water supply from AC pump powered by 2.1 kW_p solar**
 900 **array.**
 901
 902
 903
 904
 905
 906
 907
 908
 909
 910
 911
 912
 913
 914
 915
 916
 917
 918
 919
 920
 921
 922
 923

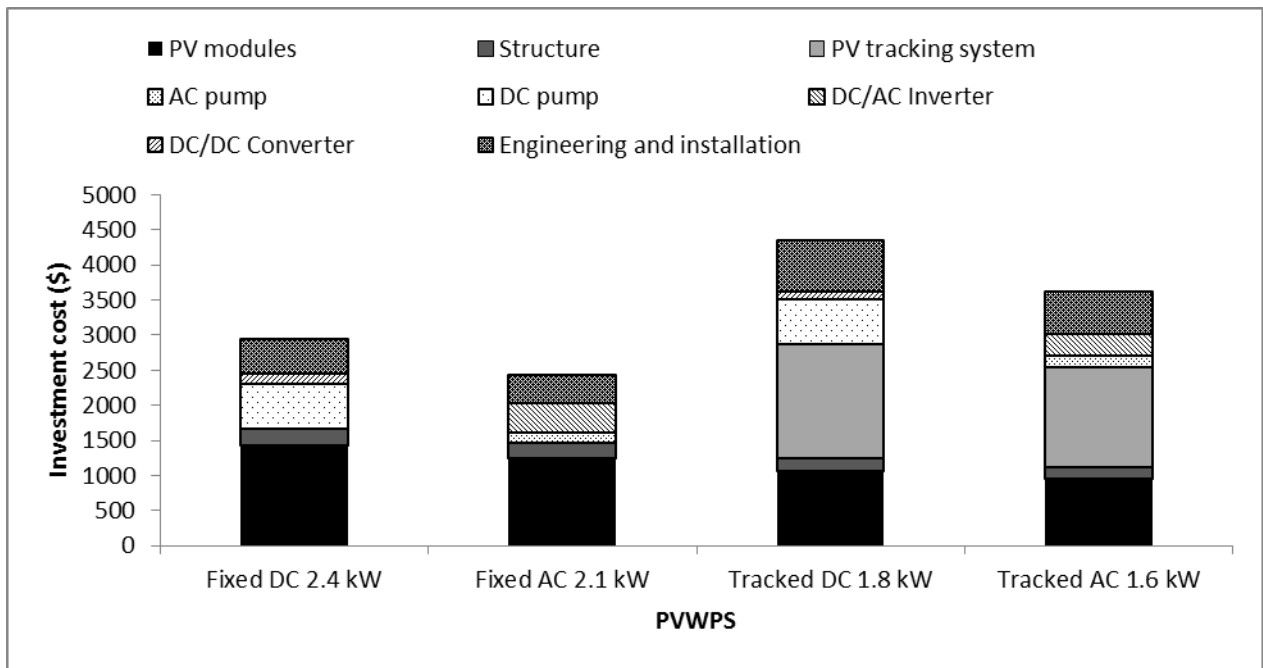


Figure 12: Total initial investment costs for the PVWPS proposed.

924
925
926
927
928
929
930
931
932
933
934
935
936
937
938
939
940
941
942
943
944
945

946 **Table captions**

947 Table 1: Climatic data for Xining.

948 Table 2: Solar energy and water demand ratio.

949 Table 3: Summary of the main system parameters and sizing results.

950 Table 4: PV water pumping system components unit costs.

951

952

953

954

955

956

957

958

959

960

961

962

963

964

965

966

967

968

969

970

971

972

973

974

975

976

977

978

Table 1: Climatic data for Xining.

	Jan	Feb	Mar	Apr	May	Jun	Jul	Aug	Sep	Oct	Nov	Dec
T (°C)	-6.0	-2.0	5.0	11.6	16.8	19.8	22.2	21.1	15.5	9.7	1.9	-4.8
RH (%)	65.6	65.0	60.5	57.6	56.5	60.6	65.5	67.4	66.9	63.6	65.3	70.2
P (mm)	0.7	3	8.3	16	33.3	37.3	50	60.2	36.6	18.7	4.5	0
WS (m/s)	2.8	3.0	3.6	3.7	3.7	3.2	3.0	2.9	2.8	2.9	3.1	2.9
GH (kWh/m ²)	75.6	96.6	144.3	168.5	182.2	187.2	184.5	157.7	127.5	89.3	76.1	53.5
EX (kWh/m ²)	149.8	176.3	253.0	297.8	344.6	346.7	349.7	319.4	262.8	212.8	156.9	136.8
LI (kWh/m ²)	160.9	156.4	195.4	210.8	239.0	247.2	269.0	267.1	235.9	219.5	184.0	170.6
LO (kWh/m ²)	209.3	204.3	254.6	272.5	303.3	306.6	326.0	319.6	285.5	269.4	232.2	212.9

979

980

981

982

983

984

985

986

987

988

989

990

991

992

993

994

995

996

997

998

999

1000

1001

1002

1003
1004
1005
1006
1007
1008
1009
1010
1011
1012
1013
1014
1015
1016
1017
1018
1019
1020
1021
1022
1023
1024
1025
1026
1027
1028
1029
1030
1031

Table 2: Solar energy and water demand ratio.

	May	June	July	Aug	Sept
I_{tot} (kWh/m ² day)	5.9	6.0	5.8	5.7	4.6
W_g (m ³ /ha day)	10.4	47.1	42.0	27.0	20.1
Ratio (%)	56.7	12.9	14.4	21.1	22.8

1032

Table 3: Summary of the main system parameters and sizing results.

Water demand (m3/ha/day)	47.1		
Irrigated area (ha)	1		
Daily operating hours	8.5		
Total dynamic head (m)	40		
Pump power (kW)	1.5		
Average monthly daily solar radiation on fixed system (kWh/m ²)	6.0		
Average monthly daily solar radiation on tracking system (kWh/m ²)	7.8		
PV module efficiency in STC (%)	14.3		
NOCT (°C)	47.2		
Power temperature coefficient (%/°C)	-0.45		
Efficiency of the system (%)	30	35	40
Fixed system power peak (kW _p)	2.8	2.4	2.1
Fixed system array area (m ²)	20	17	15
Tracking system power peak (kW _p)	2.1	1.8	1.6
Tracking system array area (m ²)	15	13	11

1033

1034

1035

1036

1037

1038

1039

1040

1041

1042

1043

1044

1045

1046

1047

1048

1049

1050

1051

Table 4: PV water pumping system components unit costs.

Component	Unit cost
PV modules	0.6 \$/W _p
Structure	0.1 \$/W _p
PV tracking system	0.9 \$/W _p
DC/AC Inverter	0.2 \$/W _p
DC/DC Converter	0.06 \$/W _p
AC pump	0.1 \$/W
DC pump	0.4 \$/W
Engineering and installation	20 % (IC)

1052